

Review

# [<sup>18</sup>F] Sodium Fluoride PET Kinetic Parameters in Bone Imaging

Tanuj Puri <sup>1</sup>, Michelle L. Frost <sup>2</sup>, Gary J. Cook <sup>3</sup> and Glen M. Blake <sup>1,\*</sup>

<sup>1</sup> Department of Biomedical Engineering, School of Biomedical Engineering and Imaging Sciences, King's College London, London SE1 7EH, UK; tanujpuri82@gmail.com

<sup>2</sup> Institute of Cancer Research Clinical Trials & Statistics Unit (ICR-CTSU), Institute of Cancer Research, Sutton SM2 5NG, UK; michelle.frost@icr.ac.uk

<sup>3</sup> Department of Cancer Imaging, School of Biomedical Engineering and Imaging Sciences, King's College London, London SE1 7EH, UK; gary.cook@kcl.ac.uk

\* Correspondence: glen.blake@kcl.ac.uk; Tel.: +44-7762717295

**Abstract:** This report describes the significance of the kinetic parameters (k-values) obtained from the analysis of dynamic positron emission tomography (PET) scans using the Hawkins model describing the pharmacokinetics of sodium fluoride ([<sup>18</sup>F]NaF) to understand bone physiology. Dynamic [<sup>18</sup>F]NaF PET scans may be useful as an imaging biomarker in early phase clinical trials of novel drugs in development by permitting early detection of treatment-response signals that may help avoid late-stage attrition.

**Keywords:** dynamic positron emission tomography; PET; computed tomography; CT; [<sup>18</sup>F] sodium fluoride; [<sup>18</sup>F]NaF; Hawkins model; kinetic modeling; bone metabolism; clinical significance



**Citation:** Puri, T.; Frost, M.L.; Cook, G.J.; Blake, G.M. [<sup>18</sup>F] Sodium Fluoride PET Kinetic Parameters in Bone Imaging. *Tomography* **2021**, *7*, 843–854. <https://doi.org/10.3390/tomography7040071>

Academic Editor: Emilio Quaia

Received: 16 September 2021

Accepted: 20 November 2021

Published: 1 December 2021

**Publisher's Note:** MDPI stays neutral with regard to jurisdictional claims in published maps and institutional affiliations.



**Copyright:** © 2021 by the authors. Licensee MDPI, Basel, Switzerland. This article is an open access article distributed under the terms and conditions of the Creative Commons Attribution (CC BY) license (<https://creativecommons.org/licenses/by/4.0/>).

## 1. Introduction

The assessment of skeletal metabolism is important for understanding the pathophysiology and for measuring the response to treatment of metabolic bone diseases such as osteoporosis [1] and for investigating and differentiating the different effects of chronic kidney disease on bone [2]. Bone biopsy is considered the gold standard for measuring bone turnover; nonetheless, it is limited to a single biopsy site at the iliac crest, subject to large measurement errors and is invasive and uncomfortable for the patient [2–8]. Moreover, multiple biopsies are required to assess treatment response and disease progression. The most commonly used and practical method is the measurement of bone turnover markers in serum and urine, which can show a large and rapid response within weeks of the commencement of treatment for osteoporosis [9,10]. However, they only provide information about global skeletal bone turnover throughout the entire skeleton [11–14]. Hence, the use of the noninvasive functional imaging technique of positron emission tomography (PET) using [<sup>18</sup>F] sodium fluoride ([<sup>18</sup>F]NaF) tracer to understand regional bone physiology, such as bone formation and perfusion [15], is attractive. The use of [<sup>18</sup>F]NaF has been validated by comparison with measurements from bone biopsy [2,16], and therefore has the potential to be used as an imaging biomarker for testing new hypotheses in clinical trials and research studies or as a clinical decision-making tool for use in healthcare [17] after standardization via multicenter trials.

The fluorine-18-fluoride ion is an excellent bone imaging tracer that is extracted by the skeletal system in proportion to bone blood flow and bone metabolism at the sites of newly formed bone. A tracer is a substance that traces a physiologic or biochemical process. Tracers are small or larger molecules (e.g., antibodies or peptides) that are labeled with radionuclides. The labeled molecules are called radiotracers or radiopharmaceuticals [18]. The use of the fluorine-18-fluoride ion as a bone imaging tracer was first introduced by Blau et al. [19]. Other bone-seeking radiotracers include the technetium-99m diphosphate bone scan agents and radionuclides of calcium and strontium, such as <sup>47</sup>Ca and <sup>85</sup>Sr formerly used for tracer kinetic studies [20]. There are no radionuclides of calcium or

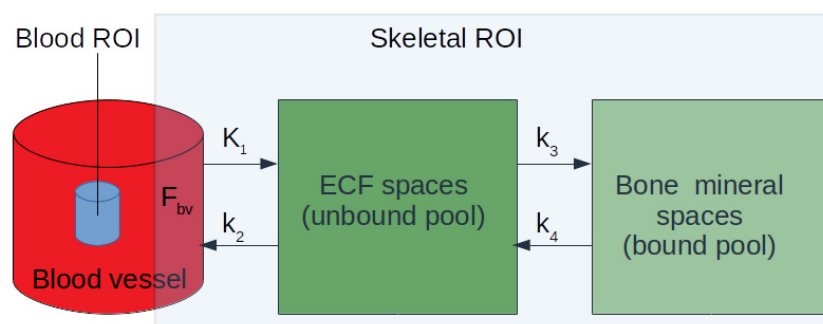
strontium with gamma ray or positron emissions suitable for imaging studies, but even if there were, the slow clearance of these elements from soft tissue due to protein binding and high renal tubular reabsorption (Ca: 99%; Sr: 97%) renders them unsuitable for this application. The gamma camera bone scan agent technetium-99m methylene diphosphonate ( $[^{99m}\text{Tc}]\text{MDP}$ ) also shows significant protein binding (20% soon after injection, rising to 60% by 4 h), but free (i.e., unbound)  $[^{99m}\text{Tc}]\text{MDP}$  is cleared through the kidneys by glomerular filtration and this aids the rapid clearance of tracer from soft tissue facilitating a clear image of the skeleton by 4 h after injection [21,22]. As a bone imaging agent,  $[^{18}\text{F}]\text{NaF}$  has the advantage of a higher clearance rate to bone than  $[^{99m}\text{Tc}]\text{MDP}$  and no protein binding to delay renal clearance from soft tissue [20], resulting in high quality bone scan images at 1 h after injection. There is some degree of reabsorption in the kidneys that varies with urine flow rate, but this is not a serious problem in a well-hydrated patient [20,21].

Bone-seeking tracers are taken up by the newly forming hydroxyapatite crystals at sites of bone formation [23–25]. The quantitative uptake of these tracers measured on images is also sometimes referred to as bone turnover or bone remodeling, even though the two processes are not the same [26]. Bone remodeling is an active process referring to the metabolic activity in the bone, characterized by a tightly coupled cyclic process between osteoblasts, osteoclasts, and osteocytes to remove old bone and replace it with new [27–29]. Bone remodeling increases in women after menopause, with an increase in osteoclast activity and a decrease in bone formation rate (BFR) and osteoblast activity. On the other hand, bone turnover is defined based on bone formation rate and/or activation frequency [30,31], and considering the net effect of remodeling on bone volume that is both resorbed and formed over a period of time [32]. Low turnover is associated with reduced osteoblast and osteoclast activities, and high bone turnover is associated with increased osteoblast and osteoclast activities, for example, in adynamic and hyperparathyroid bone diseases, respectively [3]. In adults, bone turnover occurs mainly through bone remodeling [30].

The noninvasive imaging technique of  $[^{18}\text{F}]\text{NaF}$  PET can measure early response to treatment (within weeks of treatment commencement) at clinically important sites for novel drugs being developed for osteoporosis [33–37] or other metabolic bone diseases [2,3,38] and therefore can help to avoid late-stage attrition during the drug development process. It has also been used to compare bone perfusion or turnover at different clinically important skeletal sites with varying amounts of trabecular and cortical bone, to examine the fracture healing processes [39] and investigate response to treatment in metastatic bone disease [40]. The methods of measuring bone metabolism have been extended in recent years.  $K_i$  values can be obtained from whole-body static PET images acquired for diagnostic purposes in the clinic [41], as well as from dynamic scans as short as 12 min long [42] that have the potential for translation to the clinic. A recent review by Blake et al. [43] provides more details in this context.

Studies using the  $[^{18}\text{F}]\text{NaF}$  PET technique are analyzed using a Hawkins's two-tissue compartment model (Figure 1) [44] for the quantification of parameters of interest. A compartment is a volume or space within which the tracer rapidly becomes uniformly distributed and contains no significant concentration gradient. A compartment can have a physical interpretation, e.g., the intravascular blood pool, reactants and products in a chemical reaction, or substances that are separated by membranes. A less obvious physical interpretation may be a tracer that is metabolized or trapped by two different cell types in an organ, thus defining two populations of cells as separate compartments [18]. The Hawkins model describes the pharmacokinetics of  $[^{18}\text{F}]\text{NaF}$  as it clears from the plasma into the unbound bone compartment (extracellular fluid (ECF)) and then the ionic exchange of the fluoride with hydroxyl groups in hydroxyapatite on the surface of the bone matrix to form fluorapatite preferentially at sites of osteoblastic and osteoclastic activity and newly mineralizing bone [45–47], as shown in Equation (1):





Hawkins model inputs: arterial input function (i.e. blood TAC corrected for plasma concentration) and skeletal TAC

Hawkins model outputs:  $K_1$ ,  $k_2$ ,  $k_3$ ,  $k_4$ , and  $F_{bv}$

**Figure 1.** The two-tissue compartment Hawkins model was adapted from Hawkins et al. [33] and Azad et al. [34] to analyze bone studies using  $^{18}\text{F}$ NaF PET.  $K_1$  (units:  $\text{mL min}^{-1} \text{mL}^{-1}$ ) describes the unidirectional clearance of fluoride from plasma to the whole of the bone tissue,  $k_2$  (units:  $1/\text{min}$ ) describes the reverse transport of fluoride from the ECF compartment to plasma,  $k_3$  and  $k_4$  (units:  $1/\text{min}$ ) describe the forward and backward transportation of fluoride from the bone ECF to the bone mineral compartment. In order to account for vascular  $^{18}\text{F}$ NaF activity in the tissue region, a fifth parameter, fractional blood volume ( $F_{bv}$ ) is also sometimes included in the model as the time–activity curves of skeletal region of interest include small parts of blood vessels. PET = positron emission tomography; ECF = extracellular fluid.

To obtain a dynamic PET-CT scan, participants are positioned supine with the scanner start time as the reference time. A computed tomography (CT) scan is performed first, followed by a PET scan. The tracer is administered at  $t = 10$  s injected over 10 s. A 10 mL flush is injected at  $t = 20$  s injected over 10 s. The images are acquired in list mode and re-binned at different frame durations during image reconstruction, along with corrections for scatter, random, deadtime and attenuation. Ordered subset expectation maximization or filtered back projection methods in 2D/3D mode can be used for image reconstruction, even though there may be some quantitative differences between the  $K_1$  results from images reconstructed using these two methods [48]. These images are then corrected for radioactive decay and used to obtain tissue time–activity curves (TAC) and/or an image-derived arterial input function (IDAIF). The two inputs required for the Hawkins model are: (a) a TAC describing the tracer activity over time within the skeletal volume of interest (VOI) drawn on the dynamic PET scan images, and (b) an arterial input function (AIF) describing the tracer activity over time within the artery feeding the blood plasma to the skeletal VOI [18,44,49]. The AIF can be obtained in various ways, for example, by using continuous arterial blood sampling [50], venous sampling at early time points after warming the hands to  $43^\circ\text{C}$  [51,52], or using venous blood sample obtained between 30–60 min post injection to calibrate image-derived time–activity curves of the blood [36]. Our present methods depend on arterial and venous concentrations becoming equal by 30 min after tracer injection and do not require heating the hands at  $43^\circ\text{C}$  to obtain arterialized venous blood [33,36,53,54]. The blood AIF calibrated against the blood samples is then corrected for plasma-to-whole blood ratios measured from the blood data. These inputs can be fitted to the model using various different approaches [55], including nonlinear regression (NLR). The outputs of the model are individual rate constant parameters describing the transport of  $^{18}\text{F}$ NaF between the blood plasma, extracellular fluid and bone mineral compartments (Figure 1). The physiological relevance of each of these exchange parameters is described in detail in the following sections.

## 2. $K_i$

The  $K_i$  parameter represents the net plasma clearance of [ $^{18}\text{F}$ ]NaF tracer to the bone mineral space (Figure 1). It is calculated using Equation (2):

$$K_i = K_1 \times k_3 / (k_2 + k_3) \text{ mL min}^{-1} \text{ mL}^{-1} \quad (2)$$

where,  $K_i$  is the product of  $K_1$  and the fraction of the tracer that undergoes specific binding to the bone mineral [ $k_3 / (k_2 + k_3)$ ].  $K_i$  is often referred to as the plasma clearance to the bone mineral compartment, or by some authors as the bone metabolic flux [40] or rate of bone turnover [34]. It can be understood as follows: a measured value of  $K_i$  of  $0.01 \text{ mL min}^{-1} \text{ mL}^{-1}$  means that the quantity of [ $^{18}\text{F}$ ]NaF cleared to each milliliter of bone in one minute is equal to the amount of contained in 0.01 mL of plasma.

Bone histomorphometry studies following double tetracycline labeling [2,3] are an important method of validating the use of [ $^{18}\text{F}$ ]NaF PET in the investigation of metabolic bone diseases. Histomorphometric analysis provides both structural and remodeling bone parameters [30,31]. The remodeling parameters can be static or dynamic. Static remodeling parameters include osteoblast and osteoclast activities measured as a percentage of bone surface area, osteoid thickness, bone volume measured as a percentage of total tissue volume, osteoid volume measured as a percentage of bone volume, and eroded surface measured as a percentage of the bone surface. Dynamic remodeling parameters include bone formation rate and mineralizing surface, both measured as a percentage of bone surface area, activation frequency per year, and mineralization lag time [2,3].

In a bone histomorphometry study at the lumbar spine ( $L_1$ – $L_4$ ) in 26 renal dialysis patients, Aaltonen et al. [2] demonstrated strong correlations between  $K_i$  and most of the histomorphometric parameters, including activation frequency ( $r = 0.60$ ;  $p = 0.002$ ), mineralized surface per bone surface ( $r = 0.55$ ;  $p = 0.003$ ), and osteoblast per bone surface ( $r = 0.49$ ;  $p < 0.01$ ), osteoclast per bone surface ( $r = 0.62$ ,  $p < 0.001$ ), and bone formation rate per unit bone surface area ( $r = 0.63$ ;  $p < 0.001$ ). These results support an earlier study [16], which also found a significant correlation between the net uptake of fluoride ions by PET and bone formation at the iliac crest measured by histomorphometry. Therefore, in light of these results,  $K_i$  can be considered to be a measure of bone formation rate, or the bone remodeling that reflects metabolic activity, i.e., a combination of osteoblastic and osteoclastic activities. Another study by Piert et al. [56] correlated  $K_{\text{flux}}$  ( $K_{\text{flux}} = K_i \times \text{plasma concentration of stable nonradioactive fluoride}$ ) with bone mineral apposition rate (MAR). However, it is important to note that BFR seems a more appropriate variable to correlate with  $K_i$  because MAR (units:  $\mu\text{m}/\text{day}$ ) is the maximum rate of daily increment of mineralized bone seen in a section of bone studied under the microscope, while BFR is the product of MAR and the area of active bone formation. BFR takes into account the percentage of the bone surface area undergoing active mineralization in the section under study, unlike the MAR, which might be large, but may be only a single small area of bone formation in the total area under study.

Even though dynamic PET studies of bone using [ $^{18}\text{F}$ ]NaF PET are complicated by the need to obtain arterial blood information, they provide invaluable information that is not possible to obtain with the conventional standardized uptake value (SUV) commonly used to quantify PET studies. Unlike SUV, the  $K_i$  value provides a local measurement in bone independent of any physiological changes in other parts of the body and hence represents the true change occurring at the measurement site unaffected by changes at other skeletal sites. In contrast, SUV measurements are influenced by the fact that a finite amount of administered tracer is shared across many skeletal sites in the whole body, and therefore are less specific to the measurement site than  $K_i$  [57,58]. For this reason, there are circumstances, such as the investigation of treatments that have a powerful effect on whole skeleton bone metabolism or the treatment of extensive metastatic bone disease or Paget's disease, in which SUV and other types of bone uptake measurements are less reliable measures of biological change than  $K_i$ .

In osteoporosis, anabolic treatments such as teriparatide tend to increase bone formation and therefore increase  $K_i$  [36] and antiresorptive treatments such as risedronate and other bisphosphonates tend to reduce bone resorption and therefore decrease  $K_i$  [33]. This is due to the changes in the activation frequency of newly forming bone [30,31]. A reduction in the potential number of sites for bone remodeling activity associated with a reduction in bone mass (particularly the reduced mass of trabecular bone) suggests there may be a benefit in applying a correction for bone surface area [59–62]. For example, this may explain why  $K_i$  values at the lumbar spine in postmenopausal osteoporotic women were lower than in nonosteoporotic controls despite the fact that osteoporosis is associated with a state of increased bone turnover [13]. Other studies have shown that bone turnover is an independent predictor of bone loss and fracture risk in osteoporosis [1,11,63,64] and that measurements of bone turnover can predict bone loss much earlier than the actual decrease in bone mineral density (BMD) [65]. High bone turnover increases fracture risk and bone loss by increasing the remodeling activity, leading to a deterioration in local bone microarchitecture, decrease in bone quality, structural weakness and increased susceptibility to fracture [4,6–8,66]. It is important to examine changes in bone turnover in response to treatment so its role in the quality of newly formed bone is fully appreciated. Studies show that the changes in bone turnover correlate well with changes in BMD and fracture risk [11,64,67–76] and it is the changes in bone turnover rather than the increase in BMD observed with antiresorptive therapies that explain much of the reduction in osteoporotic-related fracture risk [67,68,70].

Measurements of  $K_i$  may also have a role in the investigation of metastatic bone disease. In a recent study reported by Azad et al. [40],  $K_i$  was able to differentiate clinically progressive disease and nonprogressive disease more reliably than SUV measurements after 8 weeks of endocrine treatment in bone-predominant metastatic breast cancer patients. However, the authors suggested that larger patient groups under different therapy regimes are required to validate these findings further.

### 3. $K_1$

The parameter  $K_1$  represents the [ $^{18}\text{F}$ ]NaF plasma clearance to the ECF space (Figure 1) via capillaries and is a measure of the local rate of bone perfusion. It is measured in terms of the volume of plasma cleared of tracer per unit time per volume of tissue, units:  $\text{mL min}^{-1} \text{ mL}^{-1}$ , and is related to regional blood flow by Equation (3):

$$K_1 = E \times Q \times (1 - \text{PVC}) \text{ mL min}^{-1} \text{ mL}^{-1} \quad (3)$$

where  $E$  is the unidirectional single-pass extraction efficiency of whole blood [ $^{18}\text{F}$ ]NaF, which is often assumed to approach 100% [77],  $Q$  is regional blood flow and PVC is the packed cell volume. [ $^{18}\text{F}$ ]NaF is suitable for this role because the fluoride ion has low atomic mass and is highly diffusible. At low to moderate flow rates (less than or equal to  $0.16 \text{ mL min}^{-1} \text{ mL}^{-1}$ ), the bone perfusion measured using [ $^{18}\text{F}$ ]NaF is in good agreement with measurements made using [ $^{15}\text{O}$ ]H<sub>2</sub>O, the recognized gold standard for radionuclide blood flow studies [78,79]. However, at higher blood flow there is insufficient time for the [ $^{18}\text{F}$ ]NaF tracer to equilibrate with surrounding tissues and  $K_1$  underestimates true bone perfusion.  $K_1$  values measured at skeletal sites such as the lumbar spine (which is a highly metabolically active site) in healthy or osteoporotic subjects have been shown to have values lower than  $0.16 \text{ mL min}^{-1} \text{ mL}^{-1}$  [13,34,50]. Therefore,  $K_1$  measurements of regional skeletal bone perfusion using [ $^{18}\text{F}$ ]NaF PET are usually considered a good approximation to regional bone blood flow.

Bone perfusion plays a crucial role in maintaining bone health [80–87], influencing both osteoblastic and osteoclastic activity [80,88] and bone remodeling [89], which is associated with an age-related increase in the rate of bone loss, osteoporosis and fracture risk [19,87,89,90]. Reeve et al. [89] reported a correlation between whole skeletal bone blood flow and MAR measured using bone biopsy.  $K_1$  also correlated with the skeletal influx rate of calcium in osteoporotic patients [89]. Even though the exact mechanism between bone metabolism and bone perfusion is not known, to a certain extent the impairment

in vascular nitric oxide signaling and the vasodilator prostaglandin PGI<sub>2</sub> [80,91,92] are considered responsible for the reduced bone perfusion observed with increased age.

The reduction in bone perfusion is also associated with greater bone loss [87] and there is a direct relationship between bone perfusion and bone remodeling activity [56,89]. A reduction in bone blood flow with age has been observed in osteoporotic subjects when compared with healthy controls [83,93]. Another study in postmenopausal women with and without osteoporosis in the lumbar spine [13] showed no significant differences in  $K_1$ , probably due to the large precision error in the measurement of  $K_1$  reducing the statistical power of the study to detect these differences. However, lower values of  $K_1$  were reported in the normal femoral head [94] and distal humerus [16,50] as compared to that in normal vertebra [50], which is likely to be one of the reasons for the lower bone metabolism at the hip and humerus compared to the lumbar spine. These results were supported by another study that showed lower values of  $K_1$  at the hip compared to the lumbar spine, suggesting that lower bone blood flow is an important factor explaining the differences in  $K_i$  at different skeletal sites [95]. Furthermore, the changes in marrow composition with ageing, specifically a decrease in functioning red bone marrow and its replacement by marrow fat, may be associated with reductions in bone perfusion. In adults, functioning red marrow is largely confined to the spine, and this may be a factor explaining the differences in  $K_1$  and therefore  $K_i$  between the hip and lumbar spine [95].

#### 4. $k_2$ and $k_3$

The parameters  $k_2$  and  $k_3$  describe the backward and forward rate of [<sup>18</sup>F]NaF transfer from the bone extravascular compartment to plasma and bone mineral, respectively (Figure 1). Although the exact physiological meaning of these parameters is not clear, they reflect the overall extraction efficiency of the tracer from the extravascular compartment to bone mineral. In studies measuring response to treatment, antiresorptive treatments (such as risedronate) have been shown to increase  $k_2$  [33], in turn affecting the concentration of tracer in the extravascular tissue space (Figure 1). In addition,  $k_2$  was found to be of particular interest in Pagetic bone, where the ECF compartment is considered more complicated than in normal bone [50]. Cook et al. [61] observed a lower value of  $k_2$  and a higher value of  $k_3$ , with both factors contributing to the increased bone turnover. Pagetic bone often has its marrow space replaced by fibrous tissue, and it is possible that the [<sup>18</sup>F]NaF tracer that enters the extracellular fluid space may be less available for return to plasma.

#### 5. $k_4$

The parameter  $k_4$  describes the backward rate of [<sup>18</sup>F]NaF transfer from bone mineral to the extravascular compartment (Figure 1). The nonzero value of  $k_4$  reported by many studies reflects the fact that some of the tracer in the bone mineral space is only weakly bound and can diffuse back into the ECF space. The observed values of  $k_4$  are small (typically 0.01/min), corresponding to a tracer half-life in the bone mineral space of around 70 min [53,54]. Therefore, some methods of scan analysis assume the value of  $k_4$  is zero (for example, when using Patlak analysis [96] to calculate  $K_i$ ), an assumption that can lead to the reported values of  $K_i$  being lower by up to 25%. Puri et al. [95] reported no significant differences in the  $k_4$  values measured at lumbar spine and hip. In other studies, the impact of  $k_4$  was studied from a technical perspective to correct  $K_i$  measurements for the efflux of tracer from bone [41,53,54]. These will not be discussed further here.

#### 6. $K_1/k_2$

The ratio  $K_1/k_2$  can be understood as the effective volume of distribution of tracer in the ECF space (Figure 1).  $K_1/k_2$  describes the fraction of the skeletal VOI used to create the bone tracer time activity curve occupied by the bone ECF compartment, assuming a passive diffusion of fluoride between plasma and ECF. This is not an unreasonable assumption for fluoride with such a small atomic weight. The <sup>18</sup>F<sup>-</sup> ion is also known to bind with hydrogen atoms, creating electrically neutral hydrogen fluoride (HF), which is a small and

highly diffusible molecule that is able to cross the cell membrane. The  $[^{18}\text{F}]\text{NaF}$  in the bone ECF compartment may be less available for exchange with other compartments due to binding with marrow spaces leading to limited access to the bone mineral surface [97]. A study by Cook et al. [50] reported values of  $K_1/k_2$  corresponding to 48% of VOI volume in vertebral and 34% in humeral bone, which was in concordance with the earlier estimates in canine tibiae, which were 10% for bone ECF space alone and 24% for bone marrow ECF [98]. These findings support the fact that the ECF spaces are larger in trabecular-rich bone containing more marrow than in cortical bone.

Puri et al. [95] reported three-fold lower values of  $K_i$  at the hip compared to the lumbar spine and argued that one of the reasons (other than the differences in the  $K_1$  mainly due to the differences in marrow fat composition [84]) might be the significantly larger value of  $K_1/k_2$  in vertebrae than in hip. This may be due to the presence of more functioning red marrow in the lumbar spine, where a greater volume fraction of the bone ROI may be accessible to fluoride ions than at the hip, where the bone marrow is largely fatty. This suggests the presence of a very small ECF space at the hip, which holds a relatively small amount of tracer available for uptake by bone mineral and might be an additional reason for lower  $K_i$  at the hip site. In another study, a decrease in the ratio  $K_1/k_2$  at the lumbar spine in osteoporotic subjects treated with risedronate for 6 months suggested a smaller bone ECF space after treatment, although this did not reach statistical significance [33]. The authors argued that this finding might be because of an increase in BMD at the site, which could be mainly due to the filling of the remodeling space [99,100]. The  $K_1/k_2$  parameter is also reported to be significantly greater in Pagetic bone and suggests larger bone and nonbone ECF spaces [61], which along with an increase in delivery and clearance to total bone tissue, could lead to an overall increase in clearance of  $[^{18}\text{F}]\text{NaF}$  to the bone mineral compartment.

### 7. $k_3/(k_2 + k_3)$

The ratio of  $k_3$  and  $k_2 + k_3$  represents the fraction of tracer delivered by bone blood flow to the ECF space that binds to the bone mineral compartment and is equal to  $K_i/K_1$  (Equation (2)). Puri et al. found no statistically significant differences between the values of  $k_3/(k_2 + k_3)$  at the lumbar spine and hip in healthy postmenopausal women [95]. In studies measuring response to treatment, anabolic treatments (such as teriparatide) tend to increase  $k_3/(k_2 + k_3)$  [36] and antiresorptive treatments (such as risedronate) tend to decrease  $k_3/(k_2 + k_3)$  [33], in turn affecting the fraction of tracer that underwent specific binding to bone mineral space (Figure 1). These results suggest that the ratio  $k_3/(k_2 + k_3)$  may be an alternative measure of treatment response. Considering that the ratio of the treatment response divided by the precision error was highest for  $k_3/(k_2 + k_3)$  among all the Hawkins's model parameters [43], and that this ratio represents the fraction of tracer that undergoes binding to the bone mineral and thus of treatment effect [33,34,37], the measurement of changes in  $k_3/(k_2 + k_3)$  may be considered one of the most effective means (alongside the  $K_i$  parameter) of using  $[^{18}\text{F}]\text{NaF}$  dynamic PET scans to noninvasively investigate changes in bone formation rate.

### 8. Changes in K-Parameters in Response to Treatment

Several reports have described studies using  $[^{18}\text{F}]\text{NaF}$  PET/CT to investigate the effect of osteoporosis treatments on bone turnover in postmenopausal women. Frost et al. examined the effect of 6 months treatment with the antiresorptive agent risedronate in 18 women (mean age 67 y) with low bone density at the spine or hip [33]. Mean vertebral  $K_i$  decreased by 18.4% ( $p = 0.04$ ) with a similar decrease in the bone formation marker bone-specific alkaline phosphatase. The ratio  $k_3/(k_2 + k_3)$  decreased by 18.1% ( $p = 0.02$ ) and  $k_2$  increased by 58% ( $p < 0.05$ ). No other kinetic parameters showed statistically significant changes. Subsequently, the same group examined the effect of 6 months treatment with the bone anabolic agent teriparatide (TPT) in 18 postmenopausal women with osteoporosis [36]. Mean vertebral  $K_i$  increased by 23.8% ( $p = 0.0003$ ) with a similar increase in  $k_3/(k_2 + k_3)$

( $p = 0.0006$ ). No other kinetic parameters showed statistically significant changes. Interestingly, the change in spine SUV was only 3% and was not statistically significant ( $p = 0.84$ ). However, SUV increases of 36.9% in the femoral shaft ( $p = 0.0019$ ) and total hip ( $p = 0.032$ ) were significant. As mentioned previously, this finding demonstrates the importance of measuring  $K_i$  as well as SUV in patients with areas of highly elevated bone turnover in the skeleton, whether localized as in Paget's disease [101] or extensive metastatic bone disease, or diffusely across the entire skeleton as in TPT treatment. In such patients, the arterial plasma concentration of tracer is depressed and SUV measurements can give a false impression of true regional change [58].

### 9. Precision Errors in Measuring K-Parameters

The precision error of each parameter in the Hawkins model expressed as the coefficient of variation (Table 1) and the treatment response expressed as the percentage change between baseline and 6 months after treatment with the bone anabolic agent teriparatide were presented by Blake et al. [43]. Parameters with a large response to treatment and a small precision error are the most sensitive parameters for measuring response to treatment and require the least number of subjects to reach a statistically significant difference in a drug trial. In the teriparatide study mentioned above, the only parameters with sufficient precision and treatment response to be clinically useful were  $K_i$  and  $k_3/(k_2 + k_3)$ . The limitation of the other parameters ( $K_1$ ,  $k_2$ ,  $k_3$ ,  $k_4$ , and  $F_{bv}$ ) is that their precision errors are around 30% or greater [43], which is too poor to make them useful in most studies.

**Table 1.** Precision of [ $^{18}\text{F}$ ] sodium fluoride PET kinetic parameters [43] are listed in this table. %CoV results for SUV were 11% (9–14%). %CV: coefficient of variation; 95% CI: 95% confidence interval.

	$k_1$ $\text{mL min}^{-1} \text{mL}^{-1}$	$k_2$ $\text{min}^{-1}$	$k_3$ $\text{min}^{-1}$	$k_4$ $\text{min}^{-1}$	$F_{bv}$	$k_3/(k_2 + k_3)$	$k_i$ $\text{mL min}^{-1} \text{mL}^{-1}$
%CV	36%	52%	28%	33%	55%	19%	15%
(95% CI)	(29–45%)	(42–67%)	(23–36%)	(27–42%)	(45–70%)	(15–24%)	(12–19%)

### 10. Conclusions

In conclusion, this review discusses kinetic indices obtained from dynamic [ $^{18}\text{F}$ ]NaF PET bone studies which have allowed us to understand local bone physiology at various skeletal sites at the cellular level before structural changes in bone may be detected, which may be useful for developing and testing bone-active drugs in the future.

**Author Contributions:** Conceptualization, T.P.; writing—original draft preparation, T.P.; writing—review and editing, T.P., M.L.F., G.J.C. and G.M.B.; visualization, T.P. All authors have read and agreed to the published version of the manuscript.

**Funding:** The research was supported by the National Institute for Health Research (NIHR) Biomedical Research Centre at Guy's and St Thomas' NHS Foundation Trust and King's College London. The views expressed are those of the author(s) and not necessarily those of the NHS, the NIHR or the Department of Health.

**Institutional Review Board Statement:** Not applicable.

**Informed Consent Statement:** Not applicable.

**Data Availability Statement:** Not applicable.

**Conflicts of Interest:** The authors declare no conflict of interest.

### References

1. Heaney, R.P. Is the paradigm shifting? *Bone* **2003**, *33*, 457–465. [[CrossRef](#)]
2. Aaltonen, L.; Koivuvuori, N.; Seppänen, M.; Tong, X.; Kröger, H.; Löyttyniemi, E.; Metsärinne, K. Correlation between (18)F-Sodium Fluoride positron emission tomography and bone histomorphometry in dialysis patients. *Bone* **2020**, *134*, 115267. [[CrossRef](#)]

3. Aaltonen, L.; Koivuvuori, N.; Seppänen, M.; Burton, I.S.; Kröger, H.; Löyttyneemi, E.; Metsärinne, K. Bone Histomorphometry and (18)F-Sodium Fluoride Positron Emission Tomography Imaging: Comparison Between only Bone Turnover-based and Unified TMV-based Classification of Renal Osteodystrophy. *Calcif. Tissue Int.* **2021**, *109*, 605–614. [[CrossRef](#)] [[PubMed](#)]
4. Arlot, M.; Meunier, P.J.; Boivin, G.; Haddock, L.; Tamayo, J.; Correa-Rotter, R.; Jasqui, S.; Donley, D.W.; Dalsky, G.P.; Martin, J.S.; et al. Differential effects of teriparatide and alendronate on bone remodeling in postmenopausal women assessed by histomorphometric parameters. *J. Bone Miner. Res.* **2005**, *20*, 1244–1253. [[CrossRef](#)] [[PubMed](#)]
5. Compston, E.J.; Croucher, P.I. Histomorphometric assessment of trabecular bone remodelling in osteoporosis. *Bone Miner.* **1991**, *14*, 91–102. [[CrossRef](#)]
6. Dempster, D.W.; Cosman, F.; Kurland, E.S.; Zhou, H.; Nieves, J.; Woelfert, L.; Shane, E.; Plavetić, K.; Müller, R.; Bilezikian, J.; et al. Effects of daily treatment with parathyroid hormone on bone microarchitecture and turnover in patients with osteoporosis: A paired biopsy study. *J. Bone Miner. Res.* **2001**, *16*, 1846–1853. [[CrossRef](#)] [[PubMed](#)]
7. Lindsay, R.; Zhou, H.; Cosman, F.; Nieves, J.; Dempster, D.W.; Hodsman, A.B. Effects of a one-month treatment with PTH(1-34) on bone formation on cancellous, endocortical, and periosteal surfaces of the human ilium. *J. Bone Miner. Res.* **2007**, *22*, 495–502. [[CrossRef](#)]
8. Jiang, Y.; Zhao, J.J.; Mitlak, B.H.; Wang, O.; Genant, H.K.; Eriksen, E.F. Recombinant human parathyroid hormone (1-34) [teriparatide] improves both cortical and cancellous bone structure. *J. Bone Miner. Res.* **2003**, *18*, 1932–1941. [[CrossRef](#)]
9. Glover, S.J.; Eastell, R.; McCloskey, E.V.; Rogers, A.; Garnero, P.; Lowery, J.; Belleli, R.; Wright, T.M.; John, M.R. Rapid and robust response of biochemical markers of bone formation to teriparatide therapy. *Bone* **2009**, *45*, 1053–1058. [[CrossRef](#)]
10. Garnero, P.; Shih, W.J.; Gineyts, E.; Karpf, D.B.; Delmas, P.D. Comparison of new biochemical markers of bone turnover in late postmenopausal osteoporotic women in response to alendronate treatment. *J. Clin. Endocrinol. Metab.* **1994**, *79*, 1693–1700.
11. Garnero, P.; Hausherr, E.; Chapuy, M.C.; Marcelli, C.; Grandjean, H.; Muller, C.; Cormier, C.; Bréart, G.; Meunier, P.J.; Delmas, P.D. Markers of bone resorption predict hip fracture in elderly women: The EPIDOS Prospective Study. *J. Bone Miner. Res.* **1996**, *11*, 1531–1538. [[CrossRef](#)]
12. Beck-Jensen, J.E.; Kollerup, G.; Sørensen, H.A.; Pors Nielsen, S.; Sørensen, O.H. A single measurement of biochemical markers of bone turnover has limited utility in the individual person. *Scand J. Clin. Lab. Investig.* **1997**, *57*, 351–359. [[CrossRef](#)] [[PubMed](#)]
13. Frost, M.L.; Fogelman, I.; Blake, G.M.; Marsden, P.K.; Cook, G., Jr. Dissociation between global markers of bone formation and direct measurement of spinal bone formation in osteoporosis. *J. Bone Miner. Res.* **2004**, *19*, 1797–1804. [[CrossRef](#)]
14. Lenora, J.; Norrgren, K.; Thorsson, O.; Wollmer, P.; Obrant, K.J.; Ivaska, K.K. Bone turnover markers are correlated with total skeletal uptake of <sup>99m</sup>Tc-methylene diphosphonate (<sup>99m</sup>Tc-MDP). *BMC Med. Phys.* **2009**, *9*, 3. [[CrossRef](#)] [[PubMed](#)]
15. Schiepers, C.; Nuyts, J.; Bormans, G.; Dequeker, J.; Bouillon, R.; Mortelmans, L.; Verbruggen, A.; De Roo, M. Fluoride kinetics of the axial skeleton measured in vivo with fluorine-18-fluoride PET. *J. Nucl. Med.* **1997**, *38*, 1970–1976. [[PubMed](#)]
16. Messa, C.; Goodman, W.G.; Hoh, C.K.; Choi, Y.; Nissenson, A.R.; Salusky, I.B.; Phelps, M.E.; Hawkins, R.A. Bone metabolic activity measured with positron emission tomography and [<sup>18</sup>F]fluoride ion in renal osteodystrophy: Correlation with bone histomorphometry. *J. Clin. Endocrinol. Metab.* **1993**, *77*, 949–955. [[PubMed](#)]
17. O'Connor, J.P.; Aboagye, E.O.; Adams, J.E.; Aerts, H.J.; Barrington, S.F.; Beer, A.J.; Boellaard, R.; Bohndiek, S.E.; Brady, M.; Brown, G.; et al. Imaging biomarker roadmap for cancer studies. *Nat. Rev. Clin. Oncol.* **2017**, *14*, 169–186. [[CrossRef](#)]
18. Cherry, S.R.; Sorenson, J.A.; Phelps, M.E. *Physics in Nuclear Medicine*, 4th ed.; Saunders, W.B., Ed.; Elsevier Health Sciences: Amsterdam, The Netherlands, 2012.
19. Vandyke, D.; Anger, H.O.; Yano, Y.; Bozzini, C. Bone blood flow shown with F18 and the positron camera. *Am. J. Physiol.* **1965**, *209*, 65–70.
20. Blake, G.M.; Park-Holohan, S.J.; Cook, G.J.; Fogelman, I. Quantitative studies of bone with the use of <sup>18</sup>F-fluoride and <sup>99m</sup>Tc-methylene diphosphonate. *Semin. Nucl. Med.* **2001**, *31*, 28–49. [[CrossRef](#)]
21. Park-Holohan, J.S.; Blake, G.M.; Fogelman, I. Quantitative studies of bone using (18)F-fluoride and (99m)Tc-methylene diphosphonate: Evaluation of renal and whole-blood kinetics. *Nucl. Med. Commun.* **2001**, *22*, 1037–1044. [[CrossRef](#)]
22. Moore, E.A.; Blake, G.M.; Fogelman, I. Quantitative measurements of bone remodeling using <sup>99m</sup>Tc-methylene diphosphonate bone scans and blood sampling. *J. Nucl. Med.* **2008**, *49*, 375–382. [[CrossRef](#)]
23. Guillemart, A.; Besnard, J.C.; Le Pape, A.; Galy, G.; Fetissoff, F. Skeletal uptake of pyrophosphate labeled with technetium-95m and technetium-96, as evaluated by autoradiography. *J. Nucl. Med.* **1978**, *19*, 895–899.
24. Schümichen, C.; Rempfle, H.; Wagner, M.; Hoffmann, G. The short-term fixation of radiopharmaceuticals in bone. *Eur. J. Nucl. Med.* **1979**, *4*, 423–428. [[CrossRef](#)]
25. Einhorn, A.T.; Vigorita, V.J.; Aaron, A. Localization of technetium-99m methylene diphosphonate in bone using microautoradiography. *J. Orthop. Res.* **1986**, *4*, 180–187. [[CrossRef](#)] [[PubMed](#)]
26. Parfitt, A.M. Misconceptions (2): Turnover is always higher in cancellous than in cortical bone. *Bone* **2002**, *30*, 807–809. [[CrossRef](#)]
27. Fazzalari, N.L. Bone remodeling: A review of the bone microenvironment perspective for fragility fracture (osteoporosis) of the hip. *Semin. Cell Dev. Biol.* **2008**, *19*, 467–472. [[CrossRef](#)]
28. Crockett, J.C.; Rogers, M.J.; Coxon, F.P.; Hocking, L.J.; Helfrich, M.H. Bone remodelling at a glance. *J. Cell Sci.* **2011**, *124 Pt 7*, 991–998. [[CrossRef](#)]
29. Garnero, P.; Cremers, S. *Bone Turnover Markers. Principles of Bone Biology*; Bilezikian, J.P., Martin, T.J., Clemens, T.L., Rosen, C.J., Eds.; Academic Press: Cambridge, MA, USA, 2020; pp. 1801–1832.

30. Parfitt, A.M.; Drezner, M.K.; Glorieux, F.H.; Kanis, J.A.; Malluche, H.; Meunier, P.J.; Ott, S.M.; Recker, R.R. Bone histomorphometry: Standardization of nomenclature, symbols, and units. Report of the ASBMR Histomorphometry Nomenclature Committee. *J. Bone Miner. Res.* **1987**, *2*, 595–610. [[CrossRef](#)] [[PubMed](#)]
31. Dempster, D.W.; Compston, J.E.; Drezner, M.K.; Glorieux, F.H.; Kanis, J.A.; Malluche, H.; Meunier, P.J.; Ott, S.M.; Recker, R.R.; Parfitt, A.M. Standardized nomenclature, symbols, and units for bone histomorphometry: A 2012 update of the report of the ASBMR Histomorphometry Nomenclature Committee. *J. Bone Miner. Res.* **2013**, *28*, 2–17. [[CrossRef](#)]
32. Parfitt, A.M. What is the normal rate of bone remodeling? *Bone* **2004**, *35*, 1–3. [[CrossRef](#)] [[PubMed](#)]
33. Hawkins, R.A.; Choi, Y.; Huang, S.C.; Hoh, C.K.; Dahlbom, M.; Schiepers, C.; Satyamurthy, N.; Barrio, J.R.; Phelps, M.E. Evaluation of the skeletal kinetics of fluorine-18-fluoride ion with PET. *J. Nucl. Med.* **1992**, *33*, 633–642.
34. Azad, G.K.; Siddique, M.; Taylor, B.; Green, A.; O'Doherty, J.; Gariani, J.; Blake, G.M.; Mansi, J.; Goh, V.; Cook, G.J.R. Is Response Assessment of Breast Cancer Bone Metastases Better with Measurement of (18)F-Fluoride Metabolic Flux Than with Measurement of (18)F-Fluoride PET/CT SUV? *J. Nucl. Med.* **2019**, *60*, 322–327. [[CrossRef](#)]
35. Frost, M.L.; Cook, G.J.; Blake, G.M.; Marsden, P.K.; Benatar, N.A.; Fogelman, I. A prospective study of risedronate on regional bone metabolism and blood flow at the lumbar spine measured by 18F-fluoride positron emission tomography. *J. Bone Miner. Res.* **2003**, *18*, 2215–2222. [[CrossRef](#)]
36. Frost, M.L.; Blake, G.M.; Cook, G.J.; Marsden, P.K.; Fogelman, I. Differences in regional bone perfusion and turnover between lumbar spine and distal humerus: (18)F-fluoride PET study of treatment-naïve and treated postmenopausal women. *Bone* **2009**, *45*, 942–948. [[CrossRef](#)]
37. Uchida, K.; Nakajima, H.; Miyazaki, T.; Yayama, T.; Kawahara, H.; Kobayashi, S.; Tsuchida, T.; Okazawa, H.; Fujibayashi, Y.; Baba, H. Effects of alendronate on bone metabolism in glucocorticoid-induced osteoporosis measured by 18F-fluoride PET: A prospective study. *J. Nucl. Med.* **2009**, *50*, 1808–1814. [[CrossRef](#)]
38. Frost, M.L.; Siddique, M.; Blake, G.M.; Moore, A.E.; Schleyer, P.J.; Dunn, J.T.; Somer, E.J.; Marsden, P.K.; Eastell, R.; Fogelman, I. Differential effects of teriparatide on regional bone formation using (18)F-fluoride positron emission tomography. *J. Bone Miner. Res.* **2011**, *26*, 1002–1011. [[CrossRef](#)] [[PubMed](#)]
39. Frost, M.L.; Moore, A.E.; Siddique, M.; Blake, G.M.; Laurent, D.; Borah, B.; Schramm, U.; Valentin, M.A.; Pellas, T.C.; Marsden, P.K.; et al. <sup>18</sup>F-fluoride PET as a noninvasive imaging biomarker for determining treatment efficacy of bone active agents at the hip: A prospective, randomized, controlled clinical study. *J. Bone Miner. Res.* **2013**, *28*, 1337–1347. [[CrossRef](#)] [[PubMed](#)]
40. Installé, J.; Nzeusseu, A.; Bol, A.; Depresseux, G.; Devogelaer, J.P.; Lonneux, M. (18)F-fluoride PET for monitoring therapeutic response in Paget's disease of bone. *J. Nucl. Med.* **2005**, *46*, 1650–1658.
41. Mathavan, N.; Koopman, J.; Raina, D.B.; Turkiewicz, A.; Tägil, M.; Isaksson, H. (18)F-fluoride as a prognostic indicator of bone regeneration. *Acta Biomater.* **2019**, *90*, 403–411. [[CrossRef](#)]
42. Siddique, M.; Blake, G.M.; Frost, M.L.; Moore, A.E.; Puri, T.; Marsden, P.K.; Fogelman, I. Estimation of regional bone metabolism from whole-body 18F-fluoride PET static images. *Eur. J. Nucl. Med. Mol. Imaging* **2012**, *39*, 337–343. [[CrossRef](#)] [[PubMed](#)]
43. Puri, T.; Siddique, M.M.; Frost, M.L.; Moore, A.E.B.; Blake, G.M. A Short Dynamic Scan Method of Measuring Bone Metabolic Flux Using [18F]NaF PET. *Tomography* **2021**, *7*, 623–635. [[CrossRef](#)]
44. Blake, G.M.; Puri, T.; Siddique, M.; Frost, M.L.; Moore, A.E.B.; Fogelman, I. Site specific measurements of bone formation using [(18)F] sodium fluoride PET/CT. *Quant. Imaging Med. Surg.* **2018**, *8*, 47–59. [[CrossRef](#)] [[PubMed](#)]
45. Narita, N.; Kato, K.; Nakagaki, H.; Ohno, N.; Kameyama, Y.; Weatherell, J.A. Distribution of fluoride concentration in the rat's bone. *Calcif. Tissue Int.* **1990**, *46*, 200–204. [[CrossRef](#)]
46. Grant, F.D.; Fahey, F.H.; Packard, A.B.; Davis, R.T.; Alavi, A.; Treves, S.T. Skeletal PET with 18F-fluoride: Applying new technology to an old tracer. *J. Nucl. Med.* **2008**, *49*, 68–78. [[CrossRef](#)] [[PubMed](#)]
47. Boivin, G.; Farlay, D.; Khebbab, M.T.; Jaurand, X.; Delmas, P.D.; Meunier, P.J. In osteoporotic women treated with strontium ranelate, strontium is located in bone formed during treatment with a maintained degree of mineralization. *Osteoporos. Int.* **2010**, *21*, 667–677. [[CrossRef](#)] [[PubMed](#)]
48. Wong, J.M.; Puri, T.; Siddique, M.M.; Frost, M.L.; Moore, A.E.B.; Blake, G.M.; Fogelman, I. Comparison of ordered-subset expectation maximization and filtered back projection reconstruction based on quantitative outcome from dynamic [18F]NaF PET images. *Nucl. Med. Commun.* **2021**, *42*, 699–706. [[CrossRef](#)]
49. Puri, T.; Blake, G.M.; Curran, K.M.; Carr, H.; Moore, A.E.; Colgan, N.; O'Connell, M.J.; Marsden, P.K.; Fogelman, I.; Frost, M.L. Semiautomatic region-of-interest validation at the femur in (18)F-fluoride PET/CT. *J. Nucl. Med. Technol.* **2012**, *40*, 168–174. [[CrossRef](#)]
50. Cook, G.J.; Lodge, M.A.; Blake, G.M.; Marsden, P.K.; Fogelman, I. Differences in skeletal kinetics between vertebral and humeral bone measured by 18F-fluoride positron emission tomography in postmenopausal women. *J. Bone Miner. Res.* **2000**, *15*, 763–769. [[CrossRef](#)]
51. Phelps, M.E.; Huang, S.C.; Hoffman, E.J.; Selin, C.; Sokoloff, L.; Kuhl, D.E. Tomographic measurement of local cerebral glucose metabolic rate in humans with (F-18)2-fluoro-2-deoxy-D-glucose: Validation of method. *Ann. Neurol.* **1979**, *6*, 371–388. [[CrossRef](#)] [[PubMed](#)]
52. Puri, T.; Greenhalgh, T.A.; Wilson, J.M.; Franklin, J.; Wang, L.M.; Strauss, V.; Cunningham, C.; Partridge, M.; Maughan, T. [(18)F]Fluoromisonidazole PET in rectal cancer. *EJNMMI Res.* **2017**, *7*, 78. [[CrossRef](#)]

53. Puri, T.; Blake, G.M.; Frost, M.L.; Moore, A.E.; Siddique, M.; Cook, G.J.; Marsden, P.K.; Fogelman, I.; Curran, K.M. Validation of image-derived arterial input functions at the femoral artery using 18F-fluoride positron emission tomography. *Nucl. Med. Commun.* **2011**, *32*, 808–817. [[CrossRef](#)] [[PubMed](#)]
54. Puri, T.; Blake, G.M.; Siddique, M.; Frost, M.L.; Cook, G.J.; Marsden, P.K.; Fogelman, I.; Curran, K.M. Validation of new image-derived arterial input functions at the aorta using 18F-fluoride positron emission tomography. *Nucl. Med. Commun.* **2011**, *32*, 486–495. [[CrossRef](#)]
55. Puri, T.; Blake, G.M.; Frost, M.L.; Siddique, M.; Moore, A.E.; Marsden, P.K.; Cook, G.J.; Fogelman, I.; Curran, K.M. Comparison of six quantitative methods for the measurement of bone turnover at the hip and lumbar spine using 18F-fluoride PET-CT. *Nucl. Med. Commun.* **2012**, *33*, 597–606. [[CrossRef](#)] [[PubMed](#)]
56. Piert, M.; Zittel, T.T.; Becker, G.A.; Jahn, M.; Stahlschmidt, A.; Maier, G.; Machulla, H.J.; Bares, R. Assessment of Porcine Bone Metabolism by Dynamic [18F]Fluoride Ion PET: Correlation with Bone Histomorphometry. *J. Nucl. Med.* **2001**, *42*, 1091–1100.
57. Blake, M.G.; Frost, M.L.; Fogelman, I. Quantitative radionuclide studies of bone. *J. Nucl. Med.* **2009**, *50*, 1747–1750. [[CrossRef](#)]
58. Blake, G.M.; Siddique, M.; Frost, M.L.; Moore, A.E.; Fogelman, I. Radionuclide studies of bone metabolism: Do bone uptake and bone plasma clearance provide equivalent measurements of bone turnover? *Bone* **2011**, *49*, 537–542. [[CrossRef](#)]
59. Eastell, R.; Delmas, P.D.; Hodgson, S.F.; Eriksen, E.F.; Mann, K.G.; Riggs, B.L. Bone formation rate in older normal women: Concurrent assessment with bone histomorphometry, calcium kinetics, and biochemical markers. *J. Clin. Endocrinol. Metab.* **1988**, *67*, 741–748. [[CrossRef](#)] [[PubMed](#)]
60. Garnero, P.; Sornay-Rendu, E.; Chapuy, M.C.; Delmas, P.D. Increased bone turnover in late postmenopausal women is a major determinant of osteoporosis. *J. Bone Miner. Res.* **1996**, *11*, 337–349. [[CrossRef](#)]
61. Cook, G.J.; Blake, G.M.; Marsden, P.K.; Cronin, B.; Fogelman, I. Quantification of skeletal kinetic indices in Paget’s disease using dynamic 18F-fluoride positron emission tomography. *J. Bone Miner. Res.* **2002**, *17*, 854–859. [[CrossRef](#)]
62. Mosekilde, L.; Hasling, C.; Tågehoj Jensen, P.C.; Tågehoj Jensen, F. Bisphosphonate whole body retention test: Relations to bone mineralization rate, renal function and bone mineral content in osteoporosis and metabolic bone disorders. *Eur. J. Clin. Invest.* **1987**, *17*, 530–537. [[CrossRef](#)]
63. Szulc, P.; Montella, A.; Delmas, P.D. High bone turnover is associated with accelerated bone loss but not with increased fracture risk in men aged 50 and over: The prospective MINOS study. *Ann. Rheum Dis.* **2008**, *67*, 1249–1255. [[CrossRef](#)] [[PubMed](#)]
64. Garnero, P.; Arden, N.K.; Griffiths, G.; Delmas, P.D.; Spector, T.D. Genetic influence on bone turnover in postmenopausal twins. *J. Clin. Endocrinol. Metab.* **1996**, *81*, 140–146.
65. Grados, F.; Brazier, M.; Kamel, S.; Mathieu, M.; Hurtebize, N.; Maamer, M.; Garabédian, M.; Sebert, J.L.; Fardellone, P. Prediction of bone mass density variation by bone remodeling markers in postmenopausal women with vitamin D insufficiency treated with calcium and vitamin D supplementation. *J. Clin. Endocrinol. Metab.* **2003**, *88*, 5175–5179. [[CrossRef](#)] [[PubMed](#)]
66. McClung, M.R.; San Martin, J.; Miller, P.D.; Civitelli, R.; Bandeira, F.; Omizo, M.; Donley, D.W.; Dalsky, G.P.; Eriksen, E.F. Opposite bone remodeling effects of teriparatide and alendronate in increasing bone mass. *Arch. Intern. Med.* **2005**, *165*, 1762–1768. [[CrossRef](#)]
67. Eastell, R.; Barton, I.; Hannon, R.A.; Chines, A.; Garnero, P.; Delmas, P.D. Relationship of early changes in bone resorption to the reduction in fracture risk with risedronate. *J. Bone Miner. Res.* **2003**, *18*, 1051–1056. [[CrossRef](#)]
68. Hochberg, M.C.; Greenspan, S.; Wasnich, R.D.; Miller, P.; Thompson, D.E.; Ross, P.D. Changes in bone density and turnover explain the reductions in incidence of nonvertebral fractures that occur during treatment with antiresorptive agents. *J. Clin. Endocrinol. Metab.* **2002**, *87*, 1586–1592. [[CrossRef](#)]
69. Hansen, M.A.; Overgaard, K.; Riis, B.J.; Christiansen, C. Role of peak bone mass and bone loss in postmenopausal osteoporosis: 12 year study. *BMJ* **1991**, *303*, 961–964. [[CrossRef](#)]
70. Riggs, L.B.; Melton, L.J., 3rd; O’Fallon, W.M. Drug therapy for vertebral fractures in osteoporosis: Evidence that decreases in bone turnover and increases in bone mass both determine antifracture efficacy. *Bone* **1996**, *18* (Suppl. 3), 197s–201s. [[CrossRef](#)]
71. Melton, L.J., 3rd; Khosla, S.; Atkinson, E.J.; O’Fallon, W.M.; Riggs, B.L. Relationship of bone turnover to bone density and fractures. *J. Bone Miner. Res.* **1997**, *12*, 1083–1091. [[CrossRef](#)] [[PubMed](#)]
72. Garnero, P. Markers of bone turnover for the prediction of fracture risk. *Osteoporos. Int.* **2000**, *11* (Suppl. 6), S55–S65. [[CrossRef](#)]
73. Garnero, P.; Sornay-Rendu, E.; Claustrat, B.; Delmas, P.D. Biochemical markers of bone turnover, endogenous hormones and the risk of fractures in postmenopausal women: The OFELY study. *J. Bone Miner. Res.* **2000**, *15*, 1526–1536. [[CrossRef](#)] [[PubMed](#)]
74. Bjarnason, N.H.; Sarkar, S.; Duong, T.; Mitlak, B.; Delmas, P.D.; Christiansen, C. Six and twelve month changes in bone turnover are related to reduction in vertebral fracture risk during 3 years of raloxifene treatment in postmenopausal osteoporosis. *Osteoporos. Int.* **2001**, *12*, 922–930. [[CrossRef](#)]
75. Delmas, P.D.; Recker, R.R.; Chesnut, C.H., 3rd; Skag, A.; Stakkestad, J.A.; Emkey, R.; Gilbride, J.; Schimmer, R.C.; Christiansen, C. Daily and intermittent oral ibandronate normalize bone turnover and provide significant reduction in vertebral fracture risk: Results from the BONE study. *Osteoporos. Int.* **2004**, *15*, 792–798. [[CrossRef](#)]
76. Sarkar, S.; Reginster, J.Y.; Crans, G.G.; Diez-Perez, A.; Pinette, K.V.; Delmas, P.D. Relationship between changes in biochemical markers of bone turnover and BMD to predict vertebral fracture risk. *J. Bone Miner. Res.* **2004**, *19*, 394–401. [[CrossRef](#)]
77. Wootton, R.; Doré, C. The single-passage extraction of 18F in rabbit bone. *Clin. Phys. Physiol Meas.* **1986**, *7*, 333–343. [[CrossRef](#)]

78. Piert, M.; Machulla, H.J.; Jahn, M.; Stahlschmidt, A.; Becker, G.A.; Zittel, T.T. Coupling of porcine bone blood flow and metabolism in high-turnover bone disease measured by [(15)O]H(2)O and [(18)F]fluoride ion positron emission tomography. *Eur. J. Nucl. Med. Mol. Imaging* **2002**, *29*, 907–914. [[CrossRef](#)]
79. Piert, M.; Zittel, T.T.; Machulla, H.J.; Becker, G.A.; Jahn, M.; Maier, G.; Bares, R.; Becker, H.D. Blood flow measurements with [(15)O]H2O and [18F]fluoride ion PET in porcine vertebrae. *J. Bone Miner. Res.* **1998**, *13*, 1328–1336. [[CrossRef](#)] [[PubMed](#)]
80. Prisby, R.D.; Ramsey, M.W.; Behnke, B.J.; Dominguez, J.M., 2nd; Donato, A.J.; Allen, M.R.; Delp, M.D. Aging reduces skeletal blood flow, endothelium-dependent vasodilation, and NO bioavailability in rats. *J. Bone Miner. Res.* **2007**, *22*, 1280–1288. [[CrossRef](#)]
81. McCarthy, I. The physiology of bone blood flow: A review. *J. Bone Jt. Surg. Am.* **2006**, *88* (Suppl. 3), 4–9. [[CrossRef](#)]
82. Bloomfield, A.S.; Hogan, H.A.; Delp, M.D. Decreases in bone blood flow and bone material properties in aging Fischer-344 rats. *Clin. Orthop. Relat. Res.* **2002**, *396*, 248–257. [[CrossRef](#)]
83. Griffith, J.F.; Yeung, D.K.; Antonio, G.E.; Wong, S.Y.; Kwok, T.C.; Woo, J.; Leung, P.C. Vertebral marrow fat content and diffusion and perfusion indexes in women with varying bone density: MR evaluation. *Radiology* **2006**, *241*, 831–838. [[CrossRef](#)]
84. Griffith, J.F.; Yeung, D.K.; Tsang, P.H.; Choi, K.C.; Kwok, T.C.; Ahuja, A.T.; Leung, K.S.; Leung, P.C. Compromised bone marrow perfusion in osteoporosis. *J. Bone Miner. Res.* **2008**, *23*, 1068–1075. [[CrossRef](#)]
85. Bridgeman, G.; Brookes, M. Blood supply to the human femoral diaphysis in youth and senescence. *J. Anat.* **1996**, *188* Pt 3, 611–621.
86. Eriksen, F.E.; Eghbali-Fatourehchi, G.Z.; Khosla, S. Remodeling and vascular spaces in bone. *J. Bone Miner. Res.* **2007**, *22*, 1–6. [[CrossRef](#)] [[PubMed](#)]
87. Vogt, M.T.; Cauley, J.A.; Kuller, L.H.; Nevitt, M.C. Bone mineral density and blood flow to the lower extremities: The study of osteoporotic fractures. *J. Bone Miner. Res.* **1997**, *12*, 283–289. [[CrossRef](#)] [[PubMed](#)]
88. Ralston, S.H. The Michael Mason Prize Essay 1997. Nitric oxide and bone: What a gas! *Br. J. Rheumatol.* **1997**, *36*, 831–838. [[CrossRef](#)]
89. Reeve, J.; Arlot, M.; Wootton, R.; Edouard, C.; Tellez, M.; Hesp, R.; Green, J.R.; Meunier, P.J. Skeletal blood flow, iliac histomorphometry, and strontium kinetics in osteoporosis: A relationship between blood flow and corrected apposition rate. *J. Clin. Endocrinol. Metab.* **1988**, *66*, 1124–1131. [[CrossRef](#)]
90. Alagiakrishnan, K.; Juby, A.; Hanley, D.; Tymchak, W.; Sclater, A. Role of Vascular Factors in Osteoporosis. *J. Gerontol. Ser. A* **2003**, *58*, M362–M366. [[CrossRef](#)]
91. Parfitt, A.M. The mechanism of coupling: A role for the vasculature. *Bone* **2000**, *26*, 319–323. [[CrossRef](#)]
92. Rawlinson, S.C.; El-Haj, A.J.; Minter, S.L.; Tavares, I.A.; Bennett, A.; Lanyon, L.E. Loading-related increases in prostaglandin production in cores of adult canine cancellous bone in vitro: A role for prostacyclin in adaptive bone remodeling? *J. Bone Miner. Res.* **1991**, *6*, 1345–1351. [[CrossRef](#)] [[PubMed](#)]
93. Laroche, M.; Ludot, I.; Thiechart, M.; Arlet, J.; Pieraggi, M.; Chiron, P.; Moulinier, L.; Cantagrel, A.; Puget, J.; Utheza, G.; et al. Study of the intraosseous vessels of the femoral head in patients with fractures of the femoral neck or osteoarthritis of the hip. *Osteoporos. Int.* **1995**, *5*, 213–217. [[CrossRef](#)] [[PubMed](#)]
94. Schiepers, C.; Broos, P.; Miserez, M.; Bormans, G.; De Roo, M. Measurement of skeletal flow with positron emission tomography and 18F-fluoride in femoral head osteonecrosis. *Arch. Orthop. Trauma Surg.* **1998**, *118*, 131–135. [[CrossRef](#)] [[PubMed](#)]
95. Puri, T.; Frost, M.L.; Curran, K.M.; Siddique, M.; Moore, A.E.; Cook, G.J.; Marsden, P.K.; Fogelman, I.; Blake, G.M. Differences in regional bone metabolism at the spine and hip: A quantitative study using (18)F-fluoride positron emission tomography. *Osteoporos. Int.* **2013**, *24*, 633–639. [[CrossRef](#)] [[PubMed](#)]
96. Patlak, C.S.; Blasberg, R.G. Graphical evaluation of blood-to-brain transfer constants from multiple-time uptake data. Generalizations. *J. Cereb. Blood Flow Metab.* **1985**, *5*, 584–590. [[CrossRef](#)]
97. Hosking, D.J.; Chamberlain, M.J. Studies in man with 18 F. *Clin. Sci.* **1972**, *42*, 153–161. [[CrossRef](#)]
98. Hooper, G.; McCarthy, I.; Wootton, R.; Hughes, S. *Fluid Spaces in Canine Tibia*; Williams and Wilkins: Baltimore, MD, USA, 1984.
99. Papapoulos, S. *Bisphosphonates: Pharmacology and Use in the Treatment of Osteoporosis*; Academic Press: San Diego, CA, USA, 1996.
100. Fleisch, H. *Bisphosphonates: Mechanism of Action and Clinical Use*; Academic Press: San Diego, CA, USA, 1996.
101. Gnanasegaran, G.; Moore, A.E.; Blake, G.M.; Vijayanathan, S.; Clarke, S.E.; Fogelman, I. Atypical Paget's disease with quantitative assessment of tracer kinetics. *Clin. Nucl. Med.* **2007**, *32*, 765–769. [[CrossRef](#)]